



# Calibration of sea ice drift forecasts using random forest algorithms

Cyril Palerme<sup>1</sup> and Malte Müller<sup>1</sup>

<sup>1</sup>Development Centre for Weather Forecasting, Norwegian Meteorological Institute, Oslo, Norway

**Correspondence:** Cyril Palerme (cyril.palerm@met.no)

**Abstract.** Developing accurate sea-ice drift forecasts is essential to support decision making of maritime end-users operating in the Arctic. In this study, two calibration methods have been developed for improving 10-day sea-ice drift forecasts from an operational sea-ice prediction system (TOPAZ4). The methods are based on random forest algorithms (supervised machine learning models) and have been trained using either drifting buoy or synthetic-aperture radar observations for the target variables. Depending on the calibration method, the mean absolute error is reduced, on average, between 5.9 % and 8.1 % for the direction, and between 7.1 % and 9.6 % for the speed of sea-ice drift. Overall, the algorithms trained with buoy observations have the best performances when the forecasts are evaluated using drifting buoys as reference. However, there is a large spatial variability in these results, and the algorithms trained with buoy observations have particularly poor performances for predicting the speed of sea-ice drift in the Canadian Archipelago, along the east coast of Greenland, and north of Svalbard. In these areas, the algorithms trained with SAR observations have better performances for predicting the speed of sea-ice drift.

## 1 Introduction

Due to increasing maritime traffic in the Arctic (Eriksen and Olsen, 2018; Berkman et al., 2020), there is a growing demand for reliable sea-ice information. Nevertheless, sea ice conditions in the Arctic tend to change increasingly faster due to the ongoing acceleration of sea-ice drift (Rampal et al., 2009; Spreen et al., 2011; Tandon et al., 2018; Tschudi et al., 2020). Therefore, accurate sea-ice drift forecasts are essential for predicting future sea-ice conditions, and for end-users navigating in ice-covered waters who need up-to-date information (Jeuring and Knol-Kauffman, 2019).

Sea-ice drift forecasts are operationally produced by numerical prediction systems, but are affected by biases despite the numerous efforts for improving the models (Hebert et al., 2015; Schweiger and Zhang, 2015; Rabatel et al., 2018). Sea ice drift is influenced by various sea-ice characteristics such as concentration and thickness, as well as by near-surface wind and ocean currents (Rampal et al., 2009; Spreen et al., 2011; Olason and Notz, 2014; Yu et al., 2020). The relationships between these variables and sea ice drift are complex and not linear (Yu et al., 2020). In order to improve the accuracy of sea-ice drift forecasts, we have developed two calibration methods using random forest algorithms (Breiman, 2001), which is a supervised machine learning technique suitable for assessing nonlinear relationships between a set of predictor variables and a target variable.

While random forest methods have been widely used in sea-ice remote sensing (Miao et al., 2015; Han et al., 2016; Lee et al., 2016; Gegiuc et al., 2018; Park et al., 2020), as well as in weather forecasting (Gagne et al., 2014; Ahijevych et al., 2016;



Herman and Schumacher, 2018; Loken et al., 2019; Mao and Sorteberg, 2020), there has been less interest in using random forests in sea-ice forecasting. Recently, Kim et al. (2020) developed sea-ice concentration forecasts based on random forests and convolutional neural networks, but they obtained more accurate results using convolutional neural networks. However, other machine learning and statistical methods have been used for sea-ice forecasting, particularly for predicting the sea-ice concentration and extent (Wang et al., 2016; Chi and Kim, 2017; Comeau et al., 2019; Wang et al., 2019; Fritznier et al., 2020).

The algorithms developed in this study are based on predictor variables from sea-ice forecasts produced by the Copernicus Marine Environment Monitoring Service's (CMEMS) TOPAZ4 prediction system (Sakov et al., 2012), wind forecasts from the European Centre for Medium-Range Weather Forecasts (ECMWF), and sea-ice satellite observations from the Ocean and Sea Ice Satellite Application Facility (OSI-SAF). While all the algorithms use the same predictor variables, two sets of algorithms have been developed using either drifting buoy displacements or synthetic-aperture radar (SAR) observations for the target variables. Furthermore, the evaluation of the forecasts has been performed using drifting buoy displacements for assessing the forecast errors, and using SAR observations for analyzing the spatial variability of the forecast performances.

The data and methods used in this study are presented in sections 2 and 3 respectively. In section 4, the daily SAR observations used for analyzing the spatial variability of the forecast errors, as well as for training some of the random forest algorithms, are evaluated using buoy observations. Then, the performances of the calibrated forecasts are evaluated and compared to those from the TOPAZ4 forecasts in section 4. The discussion and conclusion of this study are presented in section 5.

## 2 Data

### 2.1 Sea-ice drift observations

Satellite sea-ice drift observations from the CMEMS product named SEAICE\_GLO\_SEAICE\_L4\_NRT\_OBSERVATIONS\_011\_006 (MOSAIC version 2.0, hereafter referred as CMEMS SAR MOSAIC product) have been used for training some random forest algorithms, as well as for analyzing the spatial variability of the performances of sea-ice drift forecasts. This product provides sea-ice drift fields derived from SAR observations acquired by the Sentinel-1 satellites with a spatial resolution of 10 km and a temporal resolution of 24 hours. Only a fraction of the Arctic is covered by this product every day, and there is no observations north of 87.7°N (figure 1). It is worth noting that this product is an average of drift vectors derived from pairs of SAR images which are not necessarily acquired around midnight, and that the averaging process introduces uncertainties in the product. However, this product has the advantage of providing gridded sea-ice drift fields with fixed time spans (from midnight to midnight the next day) which are necessary for training random forest algorithms. Moreover, the fixed time spans ease the comparison between SAR observations and sea-ice drift forecasts with daily time steps.

Data from the International Arctic Buoy Programme (IAPB) have been used for training some random forest algorithms, as well as for evaluating the SAR observations and the sea-ice drift forecasts. For consistent comparisons with the SAR observations and the sea-ice drift forecasts, the speed and direction of sea-ice drift have been calculated using the geographical coordinates of the buoys at midnight (UTC). While all buoy observations located in an area with a sea-ice concentration higher



60 than 10 % (in the OSI-SAF product described in the next section) were used for training the random forest algorithms, only  
the buoys with a speed between 0.5 and 100 km per day, located in an area with a sea-ice concentration higher than 10 %, and  
further than 50 km from the coastlines were used for verification. The drift vectors from buoy observations have been projected  
onto the grid used in the TOPAZ4 system. When several buoys were located in the same grid cell, only the nearest one from  
the grid point has been taken into account. The number of buoy observations used for evaluating the forecasts during the period  
65 from June 2020 to November 2020 varies between 9352 and 9575 depending on the lead time, and has been mapped in figure  
1 b).

## 2.2 Data used for the predictor variables

Passive microwave observations of sea-ice concentration during the day preceding the forecast start date have been used as  
predictor variable in the random forest algorithms. The version 2 of the global sea ice concentration climate data record from  
70 OSI-SAF (Lavergne et al., 2019) has been used for training the algorithms. This dataset has a spatial resolution of 25 km  
and is available with a latency of 16 days. Therefore, it cannot be used for producing operational forecasts. Since June 2020,  
calibrated forecasts have been produced daily, and near-real-time sea-ice concentration products at 25-km resolution processed  
at the Norwegian Meteorological Institute from AMSR2 and SSMIS DMSP-F16, F17, and F18 sensors based on the algorithms  
introduced in Lavergne et al. (2019) have been used. The AMSR2 observations have been used when they were available, and  
75 have been replaced by SSMIS observations when they were missing.

Short-term sea ice forecasts from the TOPAZ4 prediction system (Sakov et al., 2012) have been used in the calibration  
methods developed in this study. TOPAZ4 is a coupled ice-ocean model for the Arctic ocean which provides 10-day forecasts  
at a spatial resolution of 12.5 km, as well as a reanalysis. It uses an ensemble Kalman filter to assimilate satellite sea ice  
and oceanic observations. However, while TOPAZ4 forecasts are produced daily, only the forecasts starting on Thursdays are  
80 initialized using data assimilation and stored in the long-term archive. Though the TOPAZ4 system provides forecasts with  
hourly time steps, the forecasts with daily outputs have been used here due to the 24-hour span of SAR observations. Previous  
studies have reported that the speed of sea-ice drift is overestimated in the TOPAZ4 system compared to buoy observations  
from the IAPB (Sakov et al., 2012; Xie et al., 2017).

In addition to the OSI-SAF observations and TOPAZ4 forecasts, 10-meter wind forecasts from ECMWF are also used for the  
85 predictor variables in the random forest algorithms. These forecasts have lead times up to 10 days, and during the studied period  
(2013 - 2020), the model's spatial resolution has increased from about 16 km to 9 km (<https://www.ecmwf.int/en/forecasts/documentation-and-support/changes-ecmwf-model>).



### 3 Methods

#### 3.1 Data preparation

90 In this study, the speed of sea-ice drift was determined from the great-circle distance calculated using the Haversine formula (equation 1) between the start and end locations during 24 hours. The initial bearing on the great-circle path between the start and end locations was used for the direction of sea-ice drift, and was calculated using equation 2.

$$D = 2R \arcsin \left( \sqrt{\sin^2 \left( \frac{\varphi_{end} - \varphi_{start}}{2} \right) + \cos(\varphi_{start}) \cos(\varphi_{end}) \sin^2 \left( \frac{\lambda_{end} - \lambda_{start}}{2} \right)} \right) \quad (1)$$

$$\theta = \arctan 2 \left( \sin(\lambda_{end} - \lambda_{start}) \cdot \cos(\varphi_{end}), \cos(\varphi_{start}) \cdot \sin(\varphi_{end}) - \sin(\varphi_{start}) \cdot \cos(\varphi_{end}) \cdot \cos(\lambda_{end} - \lambda_{start}) \right) \left( \frac{180}{\pi} \right) \quad (2)$$

95 In equations 1 and 2,  $R$  is the Earth's radius,  $\varphi$  and  $\lambda$  represent the latitude and the longitude, and the subscripts "start" and "end" indicate the start and end locations. Furthermore, the wind speed and direction from ECMWF forecasts were calculated using equations 3 and 4, respectively, from the mean daily  $u$  and  $v$  components ( $\bar{u}$  and  $\bar{v}$  in equations 3 and 4). The computed wind direction is not the classic meteorological wind direction (direction from which the wind is blowing), but the opposite (direction the wind is blowing to) in order to be consistent with the direction of sea-ice drift calculated using equation 2.

$$100 \quad WS = \sqrt{\bar{u}^2 + \bar{v}^2} \quad (3)$$

$$WD = \arctan 2(\bar{u}, \bar{v}) \left( \frac{180}{\pi} \right) \quad (4)$$

Then, the sea-ice drift speed and direction from SAR observations, the OSI-SAF sea-ice concentration observations, as well as the ECMWF wind forecasts have been projected onto the polar stereographic grid used in the TOPAZ4 system using nearest-neighbor interpolation.

#### 105 3.2 Development of statistical models

In order to predict independent variables, it has been chosen to forecast the direction and speed of sea-ice drift rather than the eastward and northward components. In this study, two sets of algorithms have been developed using target variables either from buoy displacements or from SAR observations. Moreover, different algorithms have been developed for predicting the direction and speed of sea-ice drift, as well as for different lead times (1 to 10 days). Therefore, 20 different models were developed using buoy displacements, and 20 other models were developed using SAR observations. Only the TOPAZ4 forecasts starting on Thursdays are stored in the long-term archive, and the algorithms have therefore been trained using weekly data.



The period from January 2018 to May 2020 was used for training the algorithms with SAR observations (the CMEMS SAR MOSAIC product has been available since January 2018). Due to the smaller number of available observations, a longer period (June 2013 to May 2020) was used for training the algorithms with buoy observations. While using a longer period increases the size of the training data sets, it can also introduce inconsistencies in the training data sets due to the constant development of the prediction systems (TOPAZ4 and ECMWF Integrated Forecasting System). In order to optimize the performances of the algorithms trained with buoy observations, several training periods have been tested (between June 2012 and May 2020), and the best results have been found using the period from June 2013 to May 2020.

For the algorithms trained with buoy observations, the data from all the grid points where buoy observations were available within the TOPAZ4 domain have been used as independent data sets in order to create a large database, which results in about  $1.7 \times 10^4$  training data sets for each model. However, a different approach has been used for the algorithms trained with SAR observations. Taking into account all the grid points where SAR observations were available in the TOPAZ4 domain would result in using many highly correlated points for training the algorithms, which increases the probability of overfitting (meaning that the models learn from noise in the training data). In order to minimize this issue, but also taking into account a sufficient number of grid points, sensitivity tests were performed. For each forecast of the training period (January 2018 - May 2020), a random selection without replacement of the grid points has been performed, and the selected grid points were added to the training data set (similar approaches were used by Gagne et al. (2014) and Loken et al. (2019) for calibrating precipitation forecasts). Random selections between 0.1 % and 100 % of the available grid points were tested, and the differences in mean absolute errors between the algorithms trained using all the available data and the algorithms trained using only a fraction of the available data were evaluated using buoy observations as reference during the period from June 2020 to November 2020 (figure 2). Overall, the best results were found by selecting 2 % of the grid points with SAR observations. Therefore, 2 % of the available grid points were used for the algorithms trained with SAR observations in this study, which results in about  $5.7 \times 10^4$  training data sets on average (between  $5.5 \times 10^4$  and  $6.0 \times 10^4$  data sets depending on lead time). Moreover, decreasing the size of the training data sets reduces the computational cost of the algorithms. Furthermore, it is worth noting that the Arctic is not uniformly covered by SAR and buoy observations (figure 1), and that different regions have therefore different weights in the development of the algorithms.

The list of predictor variables is the same for the models predicting the direction and speed of sea-ice drift. The predictor variables can be divided into three different categories. First, some geographical information has been used with the geographical coordinates of the grid points (x and y in the stereographic projection from the TOPAZ4 system), and the distance of the grid point to the nearest coastline in the TOPAZ4 system. Then, the sea-ice concentration from passive microwave observations during the day preceding the forecast start date has also been used as predictor variable. The variables from sea-ice and wind forecasts can be considered as the last category. These variables are the wind direction and speed from ECMWF forecasts, as well as the sea-ice concentration, thickness, drift speed and direction from TOPAZ4 forecasts.

Random forest algorithms consist of an ensemble of decision trees used for regression or classification tasks (Breiman, 2001). The algorithms developed here are used for regression, and are based on 100 decision trees because there were no significant improvements when using more trees. The prediction from a random forest model used for regression is the mean value of the



150 results from all decision trees. For the direction of sea-ice drift, each decision tree predicts a value between 0 and 360°. When averaging several predictions close to the northward direction, this can be an issue because values slightly higher than 0° and slightly lower than 360° can be averaged, possibly leading to a mean value close to the southward direction. In order to avoid this issue, the predictions from all decision trees were converted to complex numbers before averaging. Then, the average of complex numbers was converted into an angle in degrees. Furthermore, the calibrated forecasts have been produced where the sea-ice concentration predicted in the TOPAZ4 forecasts was larger than 10 %.

155 Sensitivity tests were performed in order to optimize some parameters of the random forest algorithms. The best results (lowest mean absolute errors) were obtained by maximizing the depth of the decision trees, and by setting the number of predictor variables considered for splitting the nodes at three. These parameters have been chosen for all the models developed.

### 3.3 Evaluation of sea-ice drift direction

160 While comparing the speed of sea-ice drift in two data sets is straightforward, caution is needed when comparing the direction of sea-ice drift in different data sets due to the circular nature of directional data. The direction errors were calculated using equation 5, where  $D_x$  and  $D_y$  are the two directions compared in degrees (between 0° and 360°). Furthermore, the correlation between different data sets has been assessed using the Pearson correlation coefficient for the speed, and using the circular correlation coefficient (equation 6) introduced by Fisher and Lee (1983) for the direction. In equation 6,  $\bar{x}$  and  $\bar{y}$  are the means of the variables  $x$  and  $y$  respectively. Similarly to the Pearson correlation coefficient, the value of the circular correlation coefficient varies between -1 and 1 (a null value indicating no correlation, 1 meaning a perfect correlation, and -1 showing a perfect anti-correlation).

$$165 \quad \Delta D = D_x - D_y \Rightarrow Error = \begin{cases} 360 - \Delta D, & \text{if } \Delta D > 180 \\ 360 + \Delta D, & \text{if } \Delta D < -180 \\ \Delta D, & \text{otherwise} \end{cases} \quad (5)$$

$$R_c = \frac{\sum_{i=1}^n \sin(x_i - \bar{x}) \sin(y_i - \bar{y})}{\sqrt{\sum_{i=1}^n \sin^2(x_i - \bar{x}) \sum_{i=1}^n \sin^2(y_i - \bar{y})}} \quad (6)$$

## 4 Results

### 4.1 Evaluation of daily SAR observations

170 The CMEMS SAR MOSAIC product provides daily averages of drift vectors derived from pairs of SAR observations. Nevertheless, the averaging process introduces uncertainties in the product because the observations are not necessarily acquired around midnight. In figure 3, this product has been compared to buoy observations during the period from January 2018 to



November 2020. The Pearson correlation coefficient is 0.78 for the speed, and the circular correlation coefficient is 0.84 for the direction. The SAR observations have relatively low biases (the mean error is 3.0 degrees for the direction and -170 meters / day for the speed). Furthermore, the mean absolute error is 21.6 degrees for the direction and 2171 meters / day for the speed (the mean speeds are 7624 and 7795 meters / day for the SAR and buoy observations respectively). The root mean square error is 36.0 degrees for the drift direction and 3677 meters / day for the drift speed. While these errors are considerable, the large number of SAR observations compared to buoy observations makes this product potentially suitable for machine learning applications. However, we consider these errors too large for evaluating the performances of the sea-ice drift forecasts using only these observations. Therefore, the performances of sea-ice drift forecasts have been evaluated using buoy observations, and the SAR observations have been used to study the spatial variability of the forecast performances.

#### 4.2 Evaluation of the random forest algorithms

The performances of the calibrated forecasts have been evaluated and compared to those from TOPAZ4 forecasts during the period from June 2020 to November 2020 using buoy observations (figures 4 and 5). The two versions of the calibrated forecasts outperform the TOPAZ4 forecasts for both the direction and speed of sea-ice drift, and for all lead times. For predicting the direction of sea-ice drift, the random forest models trained using buoy observations have the best performances for all lead times, except 10 days. On average, these models have a mean absolute error about 8.1 % lower than the TOPAZ4 forecasts (between 1.0 % and 16.6 % depending on the lead time). This is significantly better than the models trained with SAR observations which have a mean absolute error about 5.9 % lower on average than the TOPAZ4 forecasts. Moreover, the fraction of forecasts improved by the calibration is, on average, larger for the models trained with buoy observations (57.0 %) than for the models trained with SAR observations (54.8 %). Furthermore, the root mean square error is reduced by 5.4 % and 4.0 % by the calibration for the models trained with buoy and SAR observations respectively.

For the speed of sea-ice drift, the mean absolute errors are lower in the models trained with buoy observations during the first five days, relatively similar in both versions of the calibrated forecasts for lead times between six and seven days, and lower in the models trained with SAR observations for longer lead times. On average, the mean absolute error is reduced by 9.6 % and 7.1 % by the calibration for the models trained with buoy and SAR observations respectively. The fraction of forecast improved is, on average, slightly larger for the models trained with SAR observations (55.3 %) than for the models trained with buoy observations (54.9 %). However, the root mean square errors are smaller in the models trained with buoy observations for all lead times. On average, the root mean square error is reduced by 12.0 % and 6.1 % by the calibration for the models trained with buoy and SAR observations, respectively. Moreover, the correlation between the buoy observations and the calibrated forecasts is higher for the models trained with buoy observations for all lead times, except for 1 and 4 days.

The spatial variability of the fraction of forecasts improved by the calibration has been analyzed using SAR observations as reference in order to use as many observations as possible (figures 6, 7, 8, 9), though the grid points with less than 20 SAR observations during the period from June 2020 to November 2020 have been excluded from this analysis. The number of SAR observations per grid cell used for this comparison has been mapped in figure 1 d). While the two versions of the calibrated forecasts perform relatively well for predicting the direction of sea-ice drift in most of the central Arctic, they have





lower performances than TOPAZ4 in the Canadian Archipelago (figures 6 and 7). Furthermore, the models trained with buoy observations seem to perform slightly better than the models trained with SAR observations in most of the area taken into account in this analysis.

For the speed of sea-ice drift, the models trained with buoy observations have particularly poor performances compared to TOPAZ4 in the Canadian Archipelago, along the east coast of Greenland, and north of Svalbard (figure 8). The models trained with SAR observations perform better in these areas, though they also have poor performances in the Canadian Archipelago (figure 9). Most of the buoys taken into account for evaluating the forecasts in figures 4 and 5 are not located in the areas where the models trained with buoy observations have poor performances, and this likely explains the better performances of the models trained with buoy observations compared to the models trained with SAR observations in figures 4 and 5. Furthermore, in the Canadian Archipelago, sea-ice drift is more constrained by the coastlines than in most of the Arctic, and there is a lot of landfast ice (Li et al., 2019). This could explain the poor performances of the random forest models that are mainly trained in areas where the coastlines have less influence on sea-ice drift (data from the Canadian Archipelago represent about 5 % and 3 % of the training data for the models trained with SAR and buoy observations, respectively).

### 4.3 Importance of predictor variables

In order to assess the importance of each predictor variable, the algorithms using all predictor variables have been compared to algorithms in which one of the predictor variables was removed (figure 10). This experiment was performed by using only data from the training periods (June 2013 - May 2020 and January 2018 - May 2020 for the algorithms trained with buoy and SAR observations respectively). 80 % of the data sets during these periods were selected for training the algorithms, and the remaining 20 % of the data sets were used to evaluate the performances of the algorithms. The selection of the data sets used for training and evaluating the random forest models is a random process according to the forecast start date to avoid the influence of neighboring grid points with very similar conditions, and has been repeated 100 times in order to obtain reliable results. Furthermore, the algorithms were evaluated using the same product as the one used for training the random forest models (CMEMS SAR MOSAIC product for those trained with SAR observations, and IABP buoys for those trained with buoy observations). It is worth noting that this method tends to underestimate the importance of highly correlated predictors since similar information is provided to the algorithms when one of the correlated predictors is removed.

For both calibration methods, the most important variable for predicting the drift direction is the sea-ice drift direction from TOPAZ4 forecasts. Similarly, the sea-ice drift speed from TOPAZ4 is the most important variable for predicting the speed of sea-ice drift. Moreover, the ECMWF wind forecasts and the geographical coordinates in the stereographic projection used in the TOPAZ4 system also have a significant impact on the forecast errors for predicting both the direction and speed of sea-ice drift. For the algorithms predicting the speed of sea-ice drift, the mean absolute errors are also significantly reduced by adding the sea-ice thickness forecasts from TOPAZ4. Some predictor variables do not improve the forecast accuracy for all lead times. In particular, for the algorithms predicting the speed of sea-ice drift trained with buoy observations, the forecasts of wind direction and drift direction increase the mean absolute errors for five and four lead times, respectively.





## 5 Discussion and conclusion

240 The characteristics and performances of the calibrated forecasts developed in this study depend on the observations used for training the algorithms, as well as the data sets used for the predictor variables. The 24-hour mean composites of drift vectors provided by the CMEMS SAR MOSAIC product have been used for training some algorithms due to the fixed time spans of this data set, the large number of available observations, and the relatively high spatiotemporal resolution compared to sea-ice drift products developed from passive microwave observations (Lavergne et al., 2010; Girard-Ardhuin and Ezraty, 2012; 245 Tschudi et al., 2020). However, the spatial resolution (10 km) and the time spans (24 hours) of this product prevent to develop high-resolution calibrated forecasts. Furthermore, the averaging process of drift vectors introduces significant uncertainties in the product (figure 3), which represent a limitation for developing accurate calibrated forecasts. On the other hand, buoy observations are more accurate, but the relatively low number of available observations is a limitation for the development of random forest algorithms. Both methods also have common limitations such as the heterogeneous spatio-temporal sampling 250 of the buoy and SAR observations. The random forest algorithms are more influenced by areas often covered by sea-ice drift observations than by areas with a poor coverage in these observations. This could potentially explain some of the spatial variability of the performances of the calibrated forecasts. In particular, the poor performances of the calibrated forecasts compared to TOPAZ4 in the Canadian Archipelago could be partly due to local characteristics (narrow channels and presence of landfast ice) that are not often encountered in the training data sets.

255 The forecasts used for the predictor variables are produced by operational models (ECMWF Integrated Forecasting System and the TOPAZ4 prediction system) which are constantly developed. The development of these systems could affect the performances of the random forest algorithms due to changes between the different versions of the models. This issue is more important for the algorithms trained with buoy observations due to the longer period used for training these algorithms (June 2013 to May 2020). Furthermore, while only the TOPAZ4 forecasts starting on Thursdays were used for training the random 260 forest algorithms (only these forecasts are stored in the long-term archive), the operational forecasts have been produced daily. Because only the forecasts starting on Thursdays are initialized using data assimilation, this could be an issue when producing forecasts not starting on Thursdays.

Despite these limitations, it has been shown that the calibrated forecasts produced by both methods outperform the TOPAZ4 forecasts for both the direction and speed of sea-ice drift when using buoy observations as reference (figures 4 and 5). On 265 average, the mean absolute errors for the direction of sea-ice drift are 8.1 % and 5.9 % lower than in TOPAZ4 forecasts for the algorithms trained with buoy and SAR observations respectively. For the models predicting the speed of sea-ice drift, the mean absolute errors are reduced by 9.6 % and 7.1 % for the algorithms trained with buoy and SAR observations respectively. The lower errors of the algorithms trained with buoy observations, despite their smaller training data sets, show that the accuracy of the observations used for the target variables plays a crucial role in the performances of the calibrated forecasts.

270 The spatial analysis of the forecast performances using SAR observations as reference has shown that the algorithms trained with buoy observations slightly outperform the algorithms trained with SAR observations for predicting the direction of sea-ice drift in most of the area analyzed in this study (figures 6 and 7). However, for the algorithms predicting the speed of sea-ice



drift, the forecasts trained with SAR observations have better performances in most of the area analyzed in this study (figures 8 and 9). The algorithms trained with buoy observations have particularly poor performances north of Svalbard, along the east coast of Greenland, and in the Canadian Archipelago. This is likely due to the low number of buoy observations available for training the algorithms in these areas and the particular characteristics of these areas (presence of landfast ice in the Canadian Archipelago, and high sea-ice drift speed along the east coast of Greenland and north of Svalbard).

In order to reduce forecast errors from numerical prediction systems, calibration procedures can be applied, although their performances depend on the number and accuracy of the observations used as target variables. The increasing amount of satellite data available and the improvements in sea-ice remote sensing, as well as the development of new statistical approaches, enhance the potential of calibration techniques for sea-ice forecasting. This should contribute to improve the accuracy of sea-ice forecasts delivered to maritime end-users.

*Code and data availability.* Buoy observations are available on the International Arctic Buoy Programme (IAPB) website (<https://iabp.apl.uw.edu>). Synthetic-aperture radar observations and TOPAZ4 forecasts are available on the Copernicus Marine Environment Monitoring Service server (<https://resources.marine.copernicus.eu/>). The OSI-SAF sea ice concentration observations can be downloaded from the MET-Norway FTP server (<ftp://osisaf.met.no/reprocessed/ice/conc/v2p0>) until 2015, but the data after 2015 are not publicly available. A licence is needed to download the wind forecasts from the European Centre for Medium-Range Weather Forecasts (ECMWF). Furthermore, the codes used for this analysis can be made available upon request.

*Author contributions.* C.P. conducted the analysis, and wrote the majority of the manuscript. C.P. and M.M. designed the research and contributed to the discussions of the results.

*Competing interests.* The authors declare that they have no conflict of interest.

*Acknowledgements.* The authors would like to thank John Bjørnar Bremnes, Siri Sofie Eide, Roberto Saldo, and Thomas Lavergne for valuable discussions, as well as Atle Macdonald Sørensen for maintaining the production of sea-ice concentration observations from AMSR2 and SSMIS at the Norwegian Meteorological Institute. The authors received funding from the Copernicus Marine Environmental and Monitoring Service Arctic Marine Forecasting Center and IcySea project through Mercator Océan, as well as, from the SALIENSEAS project funded by the Norwegian Research Council contract number 276223. This is a contribution to the Year of Polar Prediction (YOPP), a flagship activity of the Polar Prediction Project (PPP), initiated by the World Weather Research Programme (WWRP) of the World Meteorological Organisation (WMO).



## References

- 300 Ahijevych, D., Pinto, J. O., Williams, J. K., and Steiner, M.: Probabilistic Forecasts of Mesoscale Convective System Initiation Using the Random Forest Data Mining Technique, *Weather and Forecasting*, 31, 581–599, <https://doi.org/10.1175/WAF-D-15-0113.1>, 2016.
- Berkman, P. A., Fiske, G., Røyset, J.-A., Brigham, L. W., and Lorenzini, D.: Next-Generation Arctic Marine Shipping Assessments, pp. 241–268, Springer International Publishing, [https://doi.org/10.1007/978-3-030-25674-6\\_11](https://doi.org/10.1007/978-3-030-25674-6_11), 2020.
- Breiman, L.: Random forests, *Machine learning*, 45, 5–32, 2001.
- 305 Chi, J. and Kim, H.-c.: Prediction of arctic sea ice concentration using a fully data driven deep neural network, *Remote Sensing*, 9, 1305, 2017.
- Comeau, D., Giannakis, D., Zhao, Z., and Majda, A. J.: Predicting regional and pan-Arctic sea ice anomalies with kernel analog forecasting, *Climate Dynamics*, 52, 5507–5525, 2019.
- Eriksen, T. and Olsen, Ø.: Vessel Tracking Using Automatic Identification System Data in the Arctic, pp. 115–136, Springer International  
310 Publishing, [https://doi.org/10.1007/978-3-319-78425-0\\_7](https://doi.org/10.1007/978-3-319-78425-0_7), 2018.
- Fisher, N. I. and Lee, A. J.: A correlation coefficient for circular data, *Biometrika*, 70, 327–332, <https://doi.org/10.1093/biomet/70.2.327>, 1983.
- Fritzner, S., Graverson, R., and Christensen, K. H.: Assessment of High-Resolution Dynamical and Machine Learning Models for Prediction of Sea Ice Concentration in a Regional Application, *Journal of Geophysical Research: Oceans*, 125, e2020JC016277,  
315 <https://doi.org/https://doi.org/10.1029/2020JC016277>, 2020.
- Gagne, David John, I., McGovern, A., and Xue, M.: Machine Learning Enhancement of Storm-Scale Ensemble Probabilistic Quantitative Precipitation Forecasts, *Weather and Forecasting*, 29, 1024–1043, <https://doi.org/10.1175/WAF-D-13-00108.1>, 2014.
- Gegiuc, A., Similä, M., Karvonen, J., Lensu, M., Mäkynen, M., and Vainio, J.: Estimation of degree of sea ice ridging based on dual-polarized C-band SAR data, *The Cryosphere*, 12, 343–364, <https://doi.org/10.5194/tc-12-343-2018>, 2018.
- 320 Girard-Ardhuin, F. and Ezraty, R.: Enhanced Arctic Sea Ice Drift Estimation Merging Radiometer and Scatterometer Data, *IEEE Transactions on Geoscience and Remote Sensing*, 50, 2639–2648, <https://doi.org/10.1109/TGRS.2012.2184124>, 2012.
- Han, H., Im, J., Kim, M., Sim, S., Kim, J., Kim, D.-j., and Kang, S.-H.: Retrieval of Melt Ponds on Arctic Multiyear Sea Ice in Summer from TerraSAR-X Dual-Polarization Data Using Machine Learning Approaches: A Case Study in the Chukchi Sea with Mid-Incidence Angle Data, *Remote Sensing*, 8, 57, <https://doi.org/10.3390/rs8010057>, 2016.
- 325 Hebert, D. A., Allard, R. A., Metzger, E. J., Posey, P. G., Preller, R. H., Wallcraft, A. J., Phelps, M. W., and Smedstad, O. M.: Short-term sea ice forecasting: An assessment of ice concentration and ice drift forecasts using the U.S. Navy’s Arctic Cap Nowcast/Forecast System, *Journal of Geophysical Research: Oceans*, 120, 8327–8345, <https://doi.org/10.1002/2015JC011283>, 2015.
- Herman, G. R. and Schumacher, R. S.: Money Doesn’t Grow on Trees, but Forecasts Do: Forecasting Extreme Precipitation with Random Forests, *Monthly Weather Review*, 146, 1571–1600, <https://doi.org/10.1175/MWR-D-17-0250.1>, 2018.
- 330 Jeuring, J. and Knol-Kauffman, M.: Mapping Weather, Water, Ice and Climate Knowledge & Information Needs for Maritime Activities in the Arctic. Survey Report, 2019.
- Kim, Y. J., Kim, H.-C., Han, D., Lee, S., and Im, J.: Prediction of monthly Arctic sea ice concentrations using satellite and reanalysis data based on convolutional neural networks, *The Cryosphere*, 14, 1083–1104, <https://doi.org/10.5194/tc-14-1083-2020>, <https://tc.copernicus.org/articles/14/1083/2020/>, 2020.



- 335 Lavergne, T., Eastwood, S., Teffah, Z., Schyberg, H., and Breivik, L.-A.: Sea ice motion from low-resolution satellite sensors: An alternative method and its validation in the Arctic, *Journal of Geophysical Research: Oceans*, 115, <https://doi.org/https://doi.org/10.1029/2009JC005958>, 2010.
- Lavergne, T., Sørensen, A. M., Kern, S., Tonboe, R., Notz, D., Aaboe, S., Bell, L., Dybkjær, G., Eastwood, S., Gabarro, C., Heygster, G., Killie, M. A., Brandt Kreiner, M., Lavelle, J., Saldo, R., Sandven, S., and Pedersen, L. T.: Version 2 of the EUMETSAT OSI SAF and  
340 ESA CCI sea-ice concentration climate data records, *The Cryosphere*, 13, 49–78, <https://doi.org/10.5194/tc-13-49-2019>, 2019.
- Lee, S., Im, J., Kim, J., Kim, M., Shin, M., Kim, H.-c., and Quackenbush, L.: Arctic Sea Ice Thickness Estimation from CryoSat-2 Satellite Data Using Machine Learning-Based Lead Detection, *Remote Sensing*, 8, 698, <https://doi.org/10.3390/rs8090698>, 2016.
- Li, Z., Zhao, J., Su, J., Li, C., Cheng, B., Hui, F., Yang, Q., and Shi, L.: Spatial and Temporal Variations in the Extent and Thickness of Arctic Landfast Ice, *Remote Sensing*, 12, 64, <https://doi.org/10.3390/rs12010064>, 2019.
- 345 Loken, E. D., Clark, A. J., McGovern, A., Flora, M., and Knopfmeier, K.: Postprocessing Next-Day Ensemble Probabilistic Precipitation Forecasts Using Random Forests, *Weather and Forecasting*, 34, 2017–2044, <https://doi.org/10.1175/WAF-D-19-0109.1>, 2019.
- Mao, Y. and Sorteberg, A.: Improving radar based precipitation nowcasts with machine learning using an approach based on random forest, *Weather and Forecasting*, pp. 1–51, <https://doi.org/10.1175/WAF-D-20-0080.1>, 2020.
- Miao, X., Xie, H., Ackley, S. F., Perovich, D. K., and Ke, C.: Object-based detection of Arctic sea ice and melt  
350 ponds using high spatial resolution aerial photographs, *Cold Regions Science and Technology*, 119, 211–222, <https://doi.org/https://doi.org/10.1016/j.coldregions.2015.06.014>, 2015.
- Olason, E. and Notz, D.: Drivers of variability in Arctic sea-ice drift speed, *Journal of Geophysical Research: Oceans*, 119, 5755–5775, <https://doi.org/10.1002/2014JC009897>, 2014.
- Park, J.-W., Korosov, A. A., Babiker, M., Won, J.-S., Hansen, M. W., and Kim, H.-C.: Classification of sea ice types in Sentinel-1 synthetic  
355 aperture radar images, *The Cryosphere*, 14, 2629–2645, <https://doi.org/10.5194/tc-14-2629-2020>, 2020.
- Rabatel, M., Rampal, P., Carrassi, A., Bertino, L., and Jones, C. K. R. T.: Impact of rheology on probabilistic forecasts of sea ice trajectories: application for search and rescue operations in the Arctic, *The Cryosphere*, 12, 935–953, <https://doi.org/10.5194/tc-12-935-2018>, 2018.
- Rampal, P., Weiss, J., and Marsan, D.: Positive trend in the mean speed and deformation rate of Arctic sea ice, 1979–2007, *Journal of Geophysical Research: Oceans*, 114, <https://doi.org/10.1029/2008JC005066>, 2009.
- 360 Sakov, P., Counillon, F., Bertino, L., Lisæter, K. A., Oke, P. R., and Korabely, A.: TOPAZ4: an ocean-sea ice data assimilation system for the North Atlantic and Arctic, *Ocean Science*, 8, 633–656, <https://doi.org/10.5194/os-8-633-2012>, 2012.
- Schweiger, A. J. and Zhang, J.: Accuracy of short-term sea ice drift forecasts using a coupled ice-ocean model, *Journal of Geophysical Research: Oceans*, 120, 7827–7841, <https://doi.org/10.1002/2015JC011273>, 2015.
- Spreen, G., Kwok, R., and Menemenlis, D.: Trends in Arctic sea ice drift and role of wind forcing: 1992–2009, *Geophysical Research Letters*,  
365 38, <https://doi.org/10.1029/2011GL048970>, 2011.
- Tandon, N. F., Kushner, P. J., Docquier, D., Wettstein, J. J., and Li, C.: Reassessing Sea Ice Drift and Its Relationship to Long-Term Arctic Sea Ice Loss in Coupled Climate Models, *Journal of Geophysical Research: Oceans*, 123, 4338–4359, <https://doi.org/10.1029/2017JC013697>, 2018.
- Tschudi, M. A., Meier, W. N., and Stewart, J. S.: An enhancement to sea ice motion and age products at the National Snow and Ice Data  
370 Center (NSIDC), *The Cryosphere*, 14, 1519–1536, <https://doi.org/10.5194/tc-14-1519-2020>, 2020.
- Wang, L., Yuan, X., Ting, M., and Li, C.: Predicting Summer Arctic Sea Ice Concentration Intraseasonal Variability Using a Vector Autoregressive Model, *Journal of Climate*, 29, 1529–1543, <https://doi.org/10.1175/JCLI-D-15-0313.1>, 2016.



- Wang, L., Yuan, X., and Li, C.: Subseasonal forecast of Arctic sea ice concentration via statistical approaches, *Climate Dynamics*, 52, 4953–4971, 2019.
- 375 Xie, J., Bertino, L., Counillon, F., Lisæter, K. A., and Sakov, P.: Quality assessment of the TOPAZ4 reanalysis in the Arctic over the period 1991–2013, *Ocean Science*, 13, 123–144, <https://doi.org/10.5194/os-13-123-2017>, 2017.
- Yu, X., Rinke, A., Dorn, W., Spreen, G., Lüpkes, C., Sumata, H., and Gryanik, V. M.: Evaluation of Arctic sea ice drift and its dependency on near-surface wind and sea ice conditions in the coupled regional climate model HIRHAM–NAOSIM, *The Cryosphere*, 14, 1727–1746, <https://doi.org/10.5194/tc-14-1727-2020>, 2020.

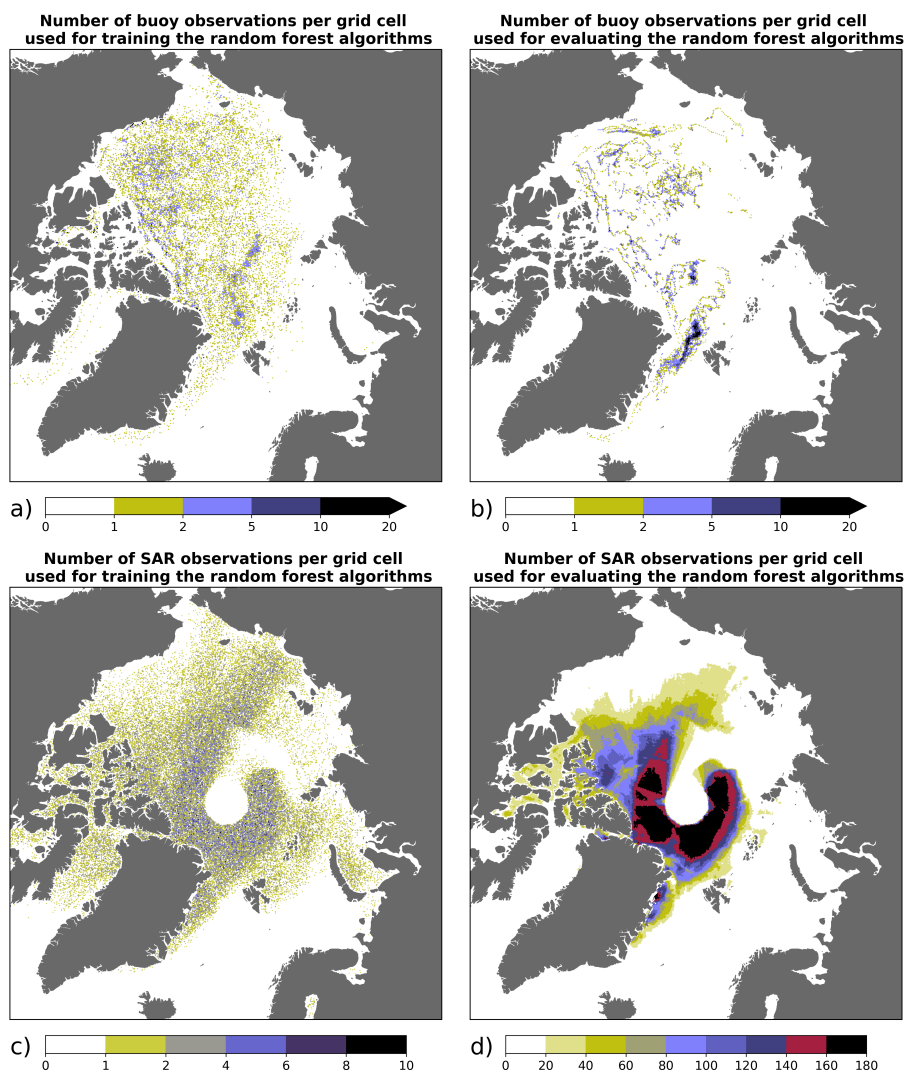


**Figure 1.** a) Number of buoy observations per grid cell used for training the random forest algorithms during the period from June 2013 to May 2020. b) Number of buoy observations per grid cell used for evaluating the random forest algorithms during the period from June 2020 to November 2020. c) Number of SAR observations per grid cell used for training the random forest algorithms during the period from January 2018 to May 2020. d) Number of SAR observations per grid cell used for evaluating the random forest algorithms during the period June 2020 to November 2020. These four maps show the number of observations for a lead time of one day (similar results have been found for other lead times).

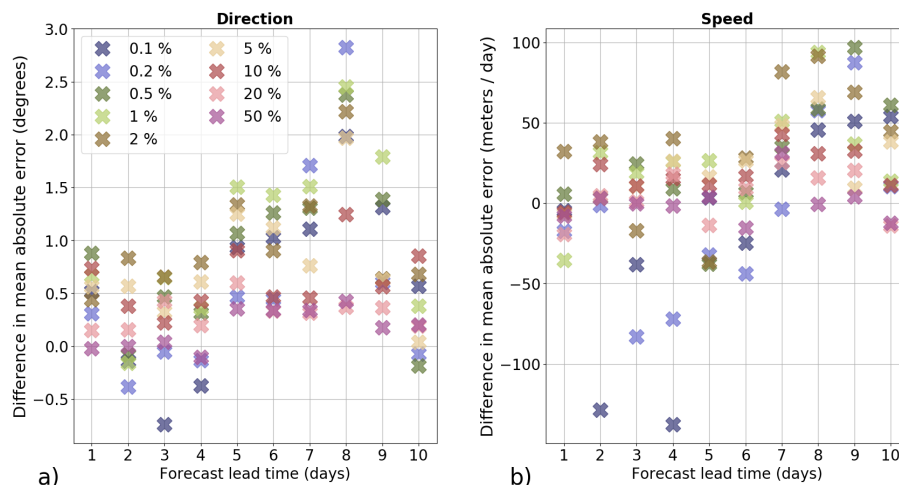


**Figure 2.** Difference in mean absolute errors during the period from June 2020 to November 2020 between the algorithms trained using all the grid points with SAR observations and the algorithms trained using only a fraction of the grid points with SAR observations for the direction (a) and the speed (b) of sea-ice drift. IAPB buoy observations have been used as reference. Positive values mean that the algorithms using only a fraction of the available grid points for training outperform the algorithms using all the available grid points. The legend from figure a) shows the fraction of grid points randomly selected for training the random forest algorithms.

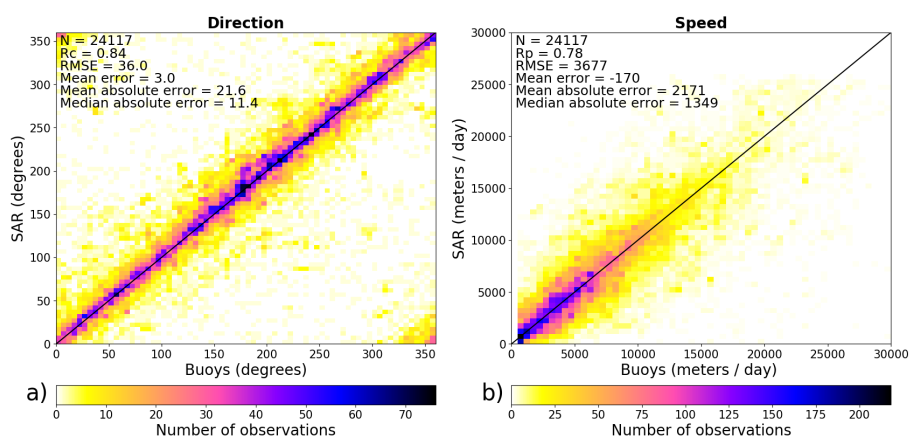


**Figure 3.** Evaluation of the CMEMS SEAICE\_GLO\_SEAICE\_L4\_NRT\_OBSERVATIONS\_011\_006 product (MOSAIC version 2.0) for the sea-ice drift direction (a) and speed (b) during the period from January 2018 to November 2020. The axes are bounded to 30 km / day for the speed for clarity, but the speed of 72 buoys exceed 30 km / day. However, these buoys were taken into account when calculating the statistics shown on the figures (N: number of samples, Rc: circular correlation coefficient, Rp: Pearson correlation coefficient, RSME: root mean square error). The color scales represent the number of observations in each bin of 5 degrees for the direction and 500 meters / day for the speed.



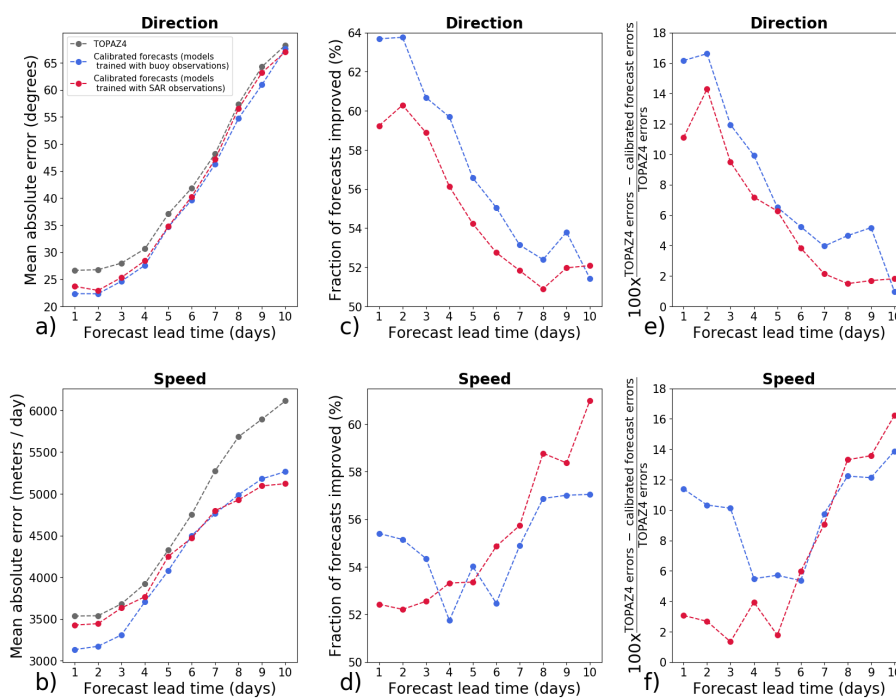


**Figure 4.** Evaluation of the performances of the calibrated forecasts and the TOPAZ4 forecasts during the period from June 2020 to November 2020. IAPB buoy observations have been used as reference. Mean absolute errors of the forecasts for the direction (a) and the speed (b), fraction of calibrated forecasts with lower absolute errors than the TOPAZ4 forecasts for the direction (c) and the speed (d). Relative improvement ( $100 \times \frac{\text{TOPAZ4 errors} - \text{calibrated forecast errors}}{\text{TOPAZ4 errors}}$ ) for the direction (e) and the speed (f).

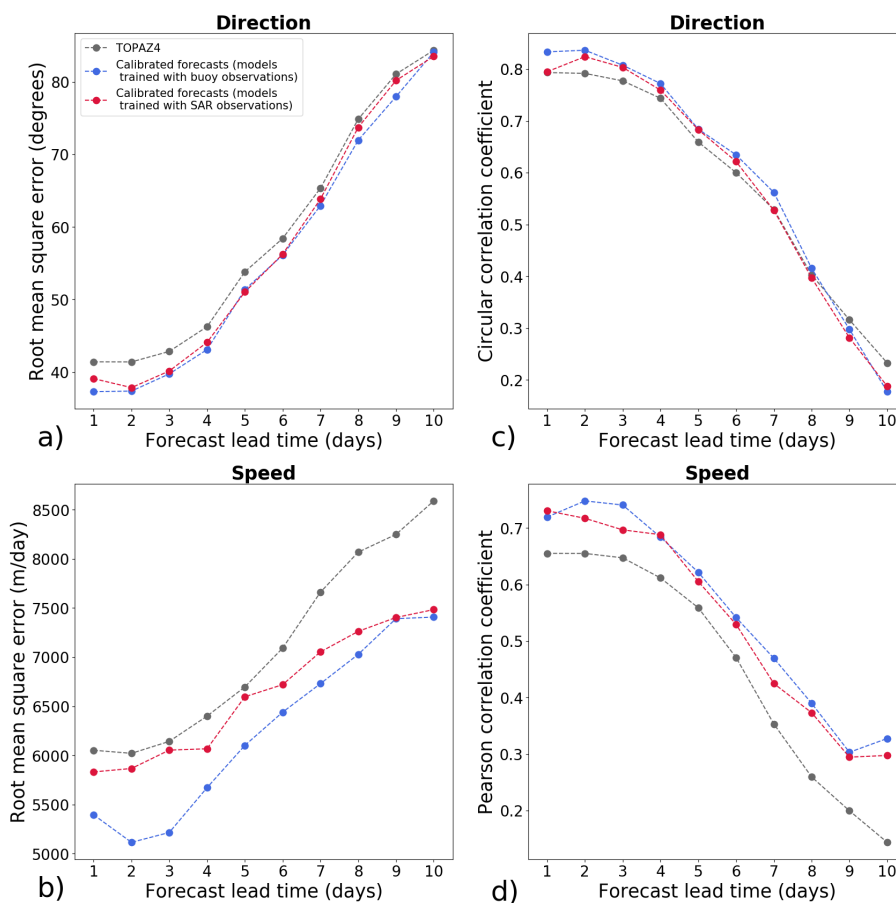


**Figure 5.** Evaluation of the performances of the calibrated forecasts and the TOPAZ4 forecasts during the period from June 2020 to November 2020. IAPB buoy observations have been used as reference. Root mean square errors of the forecasts for the direction (a) and for the speed (b), circular correlation coefficient for the direction (c) and Pearson correlation coefficient for the speed (d).

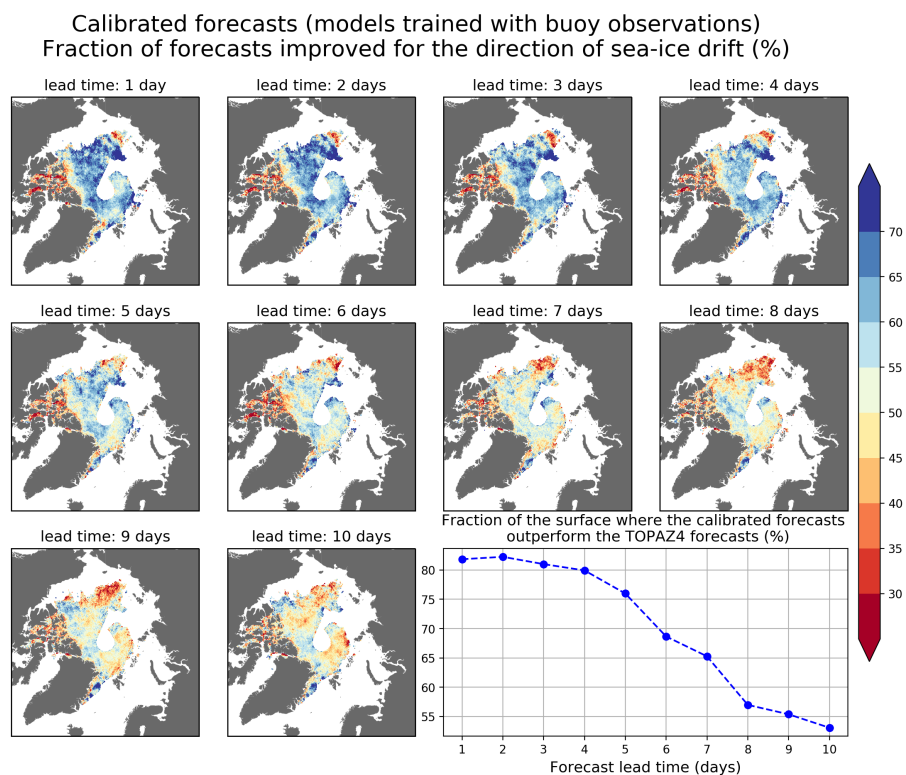


**Figure 6.** Fraction of calibrated forecasts trained using buoy observations which outperform the TOPAZ4 forecasts for the direction of sea-ice drift during the period from June 2020 to November 2020. Daily SAR observations have been used as reference. The graph in the lower right corner shows the fraction of the surface where the fraction of calibrated forecasts outperforming the TOPAZ4 forecasts is higher or equal to 50 %.

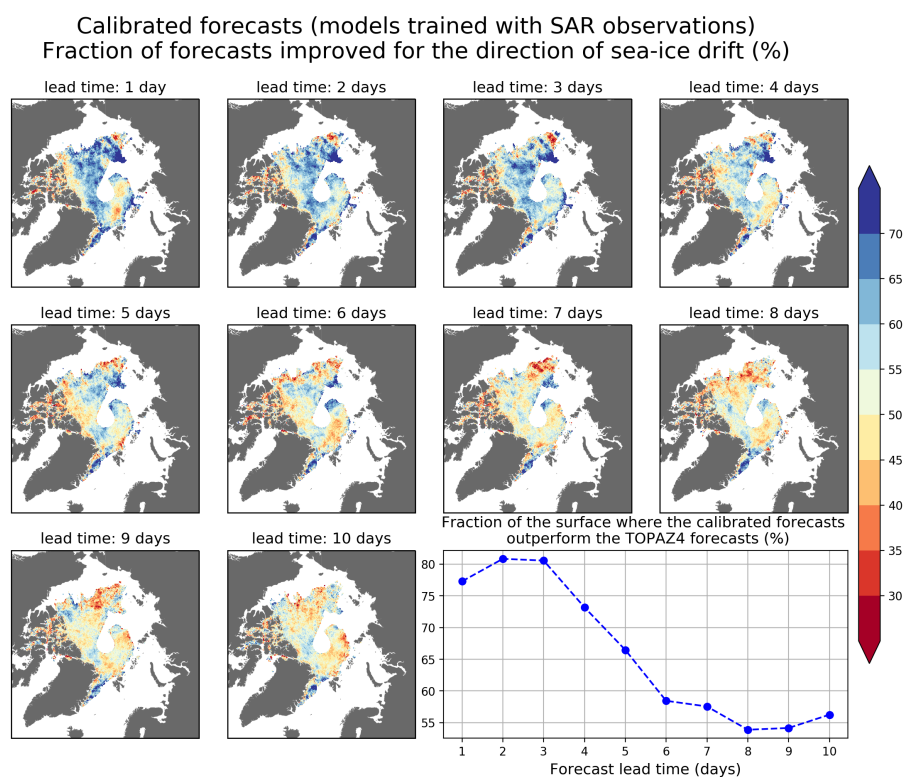


**Figure 7.** Fraction of calibrated forecasts trained using SAR observations which outperform the TOPAZ4 forecasts for the direction of sea-ice drift during the period from June 2020 to November 2020. Daily SAR observations have been used as reference. The graph in the lower right corner shows the fraction of the surface where the fraction of calibrated forecasts outperforming the TOPAZ4 forecasts is higher or equal to 50 %.

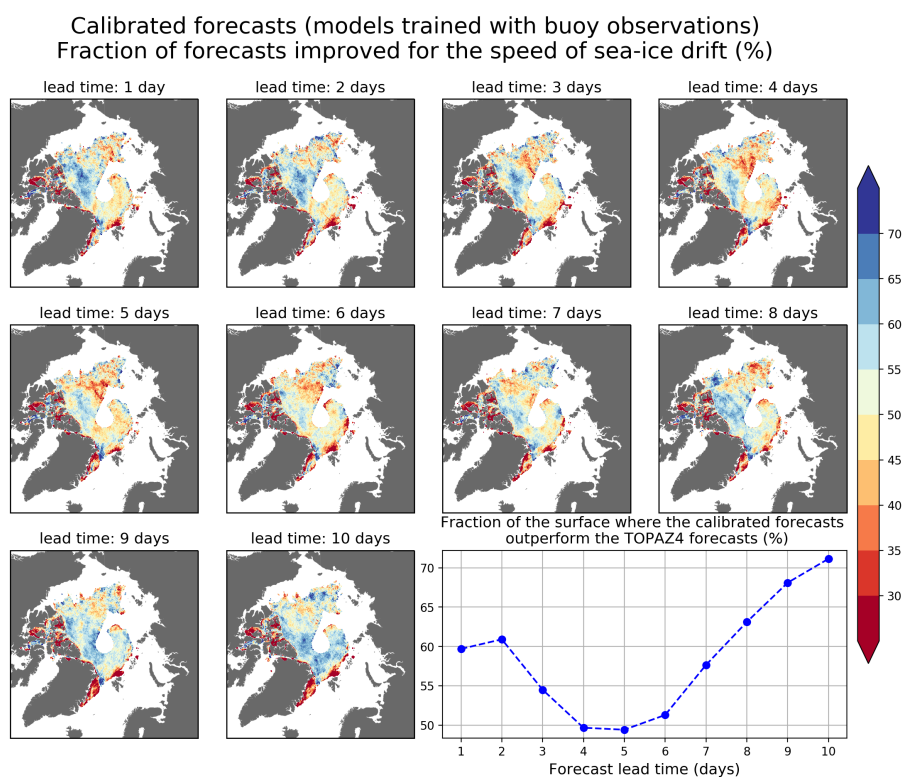


**Figure 8.** Fraction of calibrated forecasts trained using buoy observations which outperform the TOPAZ4 forecasts for the speed of sea-ice drift during the period from June 2020 to November 2020. Daily SAR observations have been used as reference. The graph in the lower right corner shows the fraction of the surface where the fraction of calibrated forecasts outperforming the TOPAZ4 forecasts is higher or equal to 50 %.

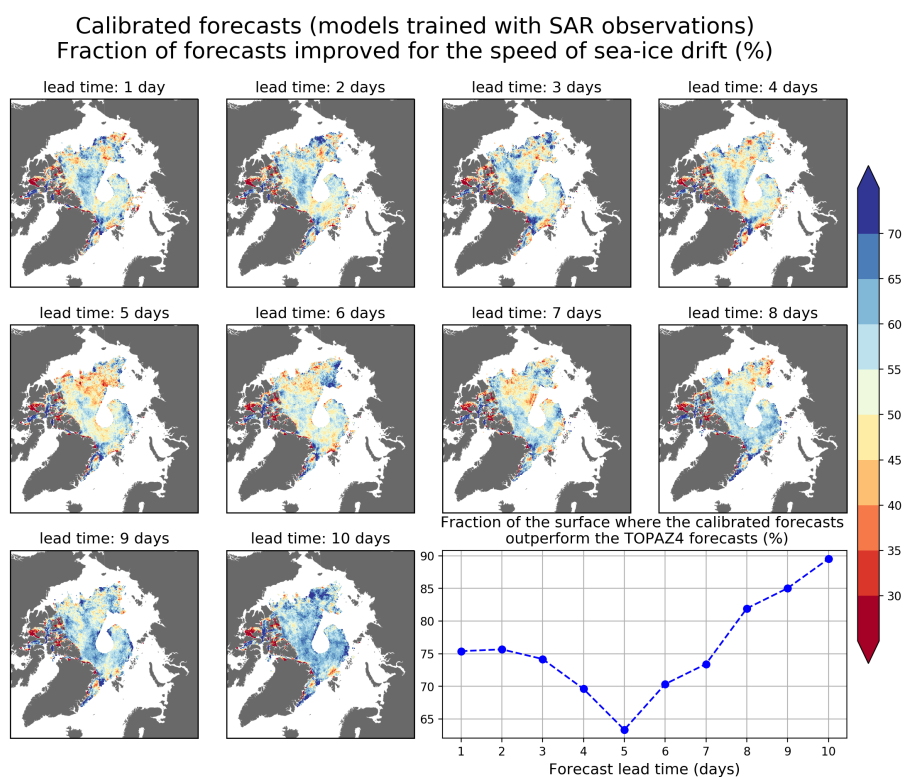


**Figure 9.** Fraction of calibrated forecasts trained using SAR observations which outperform the TOPAZ4 forecasts for the speed of sea-ice drift during the period from June 2020 to November 2020. Daily SAR observations have been used as reference. The graph in the lower right corner shows the fraction of the surface where the fraction of calibrated forecasts outperforming the TOPAZ4 forecasts is higher or equal to 50 %.

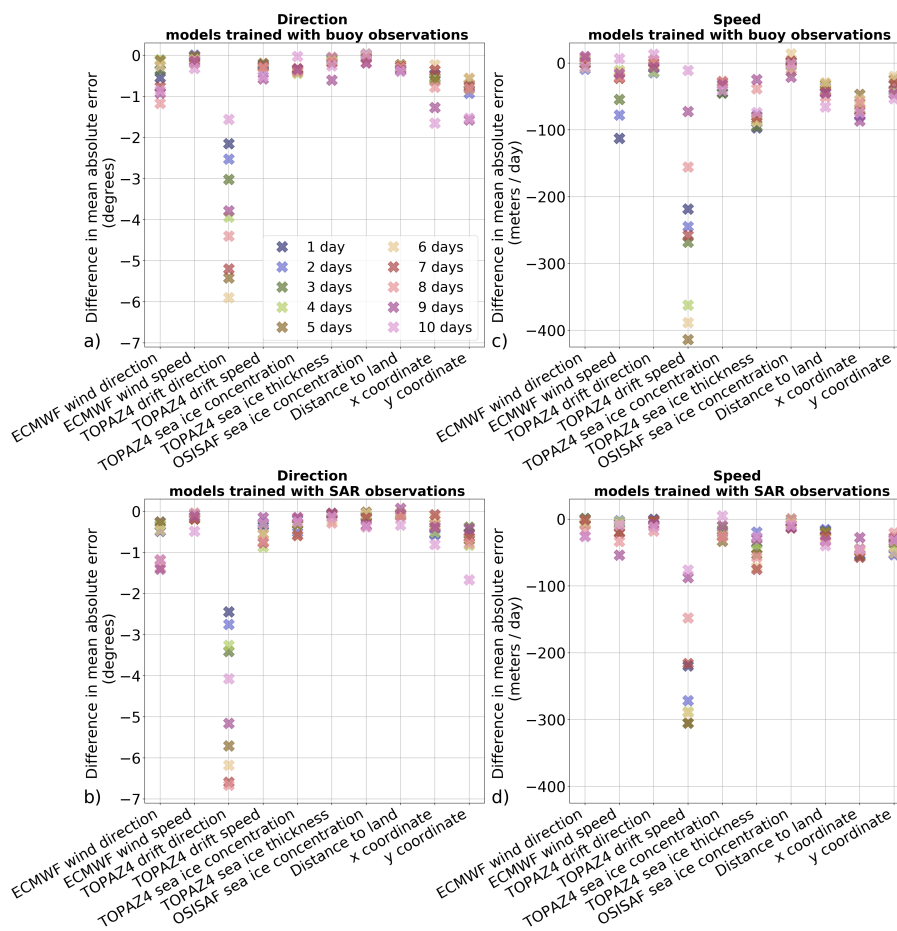


**Figure 10.** Differences in mean absolute error when one of the predictor variables is not used in the random forest algorithms for the direction (a, b) and speed (c, d) of sea-ice drift. The results are shown for the algorithms trained with buoy observations (a, c), and for the algorithms trained with SAR observations (b, d). The lead times are indicated in the legend of figure a). The differences represent the subtraction between the performances of the algorithms using all the predictor variables and the algorithms in which one predictor variable was not used. Therefore a negative value means that adding the variable in the algorithm improves the forecasts.